Journal of Materials and Environmental Science
ISSN : 2028-2508
e-ISSN : 2737-890X
CODEN : JMESCN

J. Mater. Environ. Sci., 2022, Volume 13, Issue 08, Page 884-899

http://www.jmaterenvironsci.com

Process conditions optimization of plant waste-derived microporous activated carbon using a full factorial design and genetic algorithm

Mahamane Nassirou AMADOU KIARI[1, 2], Guy Didier FANOU [1], Affoué Tindo Sylvie KONAN[3], Adama OUATTARA[1], Horo KONE[1*], Maman Mousbaou MALAM ALMA[2], Emmanuel Nogbou ASSIDJO[1], Kouassi Benjamin YAO[1]**

[1]Laboratory of Industrial Synthesis Processes, Environment and New Energies (LAPISEN), Institut National Polytechnique Félix HOUPHOUËT-BOIGNY (INP-HB), BP 1093 Yamoussoukro/Cote d'Ivoire

[2]Materials, Water and Environment Laboratory (LAMEE), Faculty of Science and Technology, Abdou Moumouni University (UAM), BP 10662 Niamey/Niger

[3]Laboratory of Thermodynamics and Physical Chemistry of the Environment (LTPCM), UFR SFA; Université Nangui Abrogoua; Abidjan/Cote d'Ivoire

**Corresponding author, Email address:horosebastien@yahoo.fr*
***Corresponding author, Email address:amadounassirou73@gmail.com*

Received 13 July 2022,
Revised 11 Aug 2022,
Accepted 12 Aug 2022

Keywords
- ✓ *Activated carbons,*
- ✓ *Two-step chemical process,*
- ✓ *Micropore optimisation,*
- ✓ *Full factorial design,*
- ✓ *Genetic algorithm.*

horosebastien@yahoo.fr
Phone: +2250576838511

Abstract

This work presents the implication of a mathematical model to prepare activated carbons from the shell of *Hyphaene Thebaica* and the seed of *Tieghmelia.* The activation of this carbon required the use of H_3PO_4 and $ZnCl_2$. For this purpose, a screening design was used to quantify the effects of the factors on the response (iodine index). The Full Factorial design via genetic algorithm provided the optimal conditions for the preparation of activated carbons. The optimal conditions were defined at a temperature of 500.850°C and a time of 4.99 hours. A microporous activated carbon was obtained with a specific surface area of 705.915 $m^2.g^{-1}$, a total pore volume of 0.906 $cm^3.g^{-1}$ and an average pore diameter of 1.66 nm. The maximum capacities of 188.009 $mg.g^{-1}$ and 710.640 $mg.g^{-1}$ were obtained by methylene blue and iodine adsorption respectively. These values are significantly close to those predicted by the model which are 194.023 $mg.g^{-1}$ and 723.649 $mg.g^{-1}$.

1. Introduction

At present, waste production is becoming more and more important in the world. Indeed, waste management is one of the main problems in developing countries (DCs). The amount of waste is increasing due to the population explosion and urbanisation [1]. Of this waste, those that are biodegradable are transformed by nature. On the other hand, those that are not or are partially biodegradable instead of hardly accumulate in nature and pollute it [2]. Unfortunately most developing countries, and typical methods of waste treatment is landfilling, incineration and composting. However, these methods do not seem to be the most rational approach, due to the by-products generated during the decomposition of the wastes. To overcome this problem, researchers have found technical ways to valorise this solid waste several precursors such as plant waste are used for the production of activated

carbons. Activated carbon is a well-known material used as an adsorbent. It can be obtained from carbon-rich materials which can be of plant or mineral origin. Its surface functions and textural properties (specific surface area, pore size distribution), give it the property to adsorb [3–7]. Activated carbons can be manufactured by physical activation, chemical activation and physicochemical activation [8,9]. Nowadays, activated carbon is used in various technological processes the treatment of drinking water and wastewater, or as a catalyst in catalytic processes are some of its use [10]. A lot of research work has been done on the preparation of activated carbons. Several precursors such as plant waste as are used for the production of activated carbons. They include the shell of *Balanites Aegyptiaca*, the shell of *Zizyphus Mauritiana*, the shell of *Hyphaene Thebaica*, [11], the branches or petioles of the roast palm [12,13], bamboo stalks or canes [14], *Coconut* [15], *Eucalyptus* wood [3], *Tieghmelia* seed called makoré and *Delonix* called flamboyant [16], *Parinari Macrophylla* shell [6], *Coffee residues* [17] and many others. Despite the availability of biomass in the West African region, some African countries continue to import activated carbons in large quantities for various applications including industrial wastewater treatment, mineral processing, and many others. This is why it seems that it is necessary to prepare and characterise low-cost activated carbons from locally available biomass. The general objective of this study is to optimize process conditions of a microporous activated carbon using a mathematical model. In this vein, it was decided in the present study to use *Hyphaene Thebaica* shells, *Tieghmelia* seeds, *Hyphaene Thebaica* and *Tieghmelia* to produce activated carbon. The use of these materials in this work has a double interest:

(i) to develop low cost activated carbons,

(ii) to valorise this category of waste in order to give it added value.

The originality of this work is to optimize the micropores and minimize the macropores by the full factorial design via the genetic algorithm by the two-step chemical method of activations with orthophosphoric acid (H_3PO_4) as activating agent.

2. Material and methods

2.1 Reagents

The reagents used in this work are shown in **table 1.**

Chemical products	Purity	Sources
Orthophosphoric acid (H_3PO_4) Molar mass = 98 g/mol, density = 1.70	85 %	Merck
Zinc chloride ($ZnCl_2$) Molar mass = 136.28 g/mol	98.2%	Merck
Methylene blue ($C_{16}H_{18}ClN_3S$) Molar mass = 319.86 g/mol		Sigma-Aldrich
Iodine 1 N		
Sodium thiosulphate ($Na_2S_2O_3.5H_2O$) Molar mass = 248.18 g/mol, 0.1 N		Sigma-Aldrich

2.2 Plant material

The shells of *Hyphaene thebaica* (Figure 1a) and *Tieghmelia* seeds (Figure 1b) were used to prepare the activated carbons. The doum palm or *Hyphaene Thebaica* and the Makore or *Tieghmelia* are native

to West Africa. *Hyphaene thebaica* shells and *Tieghmelia* seeds are difficult to biodegrade, which is an environmental problem.

(1a) (1b)

Figure 1 : Shells of *Hyphaene Thebaica* (1a) and *Tieghmelia* seeds (1b)

Hyphaene Thebaica shells were collected from a dump in the Niamey-Niger katako market and *Tieghmelia* seeds from the west of Cote d'Ivoire. They were then pitted, crushed, washed with tap water to remove dust, washed with distilled water and oven dried at 105°C for 24 hours. Figure 2 shows the resulting materials.

(2a) (2b)

Figure 2: *Hyphaene thebaica* (BHT) (2a) and *Tieghmelia* (BMC) (2b) raw materials

2.3 Methods

2.3.1 Preparation of activated carbons

For the preparation of the coals, two experimental designs were used: a Hadamard design and a Full Factorial design. The method used is two-step activation [8,9,18,19]. The impregnation consisted of putting 24 g of raw material in 100 mL of the activating agent at a given concentration. The mixture was stirred at room temperature for 12 or 24 hours. After stirring the mixture was recovered by filtration, dried at 105 °C for 24 h and then activated at a fixed temperature for a given time. After cooling, the materials obtained were washed abundantly with distilled water until the pH of the rinsing water was between 6.5 and 7, then dried in an oven at 105°C for 24 h. The activated carbons thus obtained were ground and then sieved to obtain grains with a size of 500µm or less.

2.3.2 Experimental design methodology

2.3.2.1 Hadamard Plan

First, a screening design was used to quantify the effects of the factors on the response under study (the Iodine Index). Table 2 shows the experimental range of the variable factors. Table 3 gives the Hadamard matrix with the coded variables -1 and +1 and the experimental design by replacing the variables coded -1 and +1 with the corresponding real variables.

Table 2: Experimental area

Factors	Level -1	Level +1
X_1 : Raw materials	Makoré (BMC)	*Hyphaene Thebaiqqca* (BHT)
X_2 : Activating agents	$Zncl_2$	H_3PO_4
X_3 : Concentration	1 M	3 M
X_4 : Soaking time	12 H	24 H
X_5 : Temperature	500 ^{0}C	700 ^{0}C
X_6 : Duration	3 h	5 h

Table 3: Experimental matrix and Experimental design

Assay N°	Experimental matrix						Experimental design					
	X_1	X_2	X_3	X_4	X_5	X_6	X_1	X_2	X_3	X_4	X_5	X_6
1	+1	+1	-1	+1	-1	-1	BHT	H_3PO_4	1	24	500	3
2	-1	+1	+1	-1	+1	-1	BMC	H_3PO_4	3	12	700	3
3	-1	-1	+1	+1	-1	+1	BMC	$ZnCl_2$	3	24	500	5
4	+1	-1	+1	+1	+1	-1	BHT	$ZnCl_2$	3	24	700	3
5	-1	+1	-1	+1	+1	+1	BMC	H_3PO_4	1	24	700	5
6	+1	-1	-1	-1	+1	+1	BHT	$ZnCl_2$	1	12	700	5
7	+1	+1	+1	-1	-1	+1	BHT	H_3PO_4	3	12	500	5
8	-1	-1	-1	-1	-1	-1	BMC	$ZnCl_2$	1	12	500	3

2.3.2.2 Full Factorial Design

The Full Factorial design was used to determine the optimal conditions for the preparation of activated carbons, maximising the formation of micropores and minimising that of macropores. Table 4 shows the experimental area established.

Table 4: Experimental area of the full factorial design

Factors	Level -1	Level+1
Charring temperature (X_1)	500 °C	700 °C
Charring time (X_2)	3 h	5 h

These two (2) factors, at two levels each, result in the complete factor matrix of $2^2 = 4$. Table 5 shows the factor matrix table and the experimental design by replacing the coded values (-1 and +1) with the real values (temperature and time).

2.3.2.3 Statistical analysis

A model equation was established to analyse the correlation between the variables (X_i) and the responses (Y). Equations 1 and 2 give the form of the model equation for the Hadamard design and the full factorial design respectively. And Equations 3 and 4 give the form of the equation for the coding of the natural U and coded X variables respectively:

$$Y = b_0 + \sum_{i=1}^{n} b_i X_i \quad (1)$$

$$Y = b_0 + \sum_{i} b_i X_i + \sum_{ij} b_{ij} X_i X_j \quad (2)$$

With, b_0, the value of the average coefficient; b_i, the effect of factors X_i and b_{ij} the effect of interactions of factors i and j.

$$X_{ij} = \frac{U_{ij} - U_j^0}{\Delta U_j} \quad (3)$$

Conversely :

$$U_{ij} = U_j^0 + X_{ij}.\Delta U_j \quad (4)$$

With,

U_j^0 :Value of the natural variable j at the centre of the domain;

U_{ij} : Value of natural variable j at experiment i;

ΔU_j : No change in natural variable j;

X_{ij}: Value of coded variable j for experiment.

The processing of the results was done with the Nemrod version 2000 software.

A factor is significance if its coefficient is greater than twice its standard deviation *σ(bi)* [20–23] according to the formula 5 and 6.

$$\sigma(b_i) = \frac{\sigma_r}{\sqrt{N}} \quad (5)$$

$$\sigma_r = \sqrt{\frac{1}{N-p}\sum_{1}^{N}(Y_i - \widehat{Y}_i)^2} \quad (6)$$

Which, N is the number of assays, p is the number of coefficients, Y_i is the experimental response and $\widehat{Y}_i$ is the predicted response by model.

Table 5: Experimental matrix and Experimental design

Assay N°	Experimental matrix		Experimental design	
	X_1	X_2	X_1	X_2
1	-1	-1	500	3
2	+1	-1	700	3
3	-1	+1	500	5
4	+1	+1	700	5

2.3.3 Genetic algorithm

The overall optimisation by maximising the formation of micropores and minimising that of macropores was carried out using the genetic algorithm methodology. The latter was used to determine

the set of points of the system of equations (Pareto front), in order to have optimal conditions for the preparation of activated carbon. Figure 3 shows the flow chart of a genetic algorithm [24].

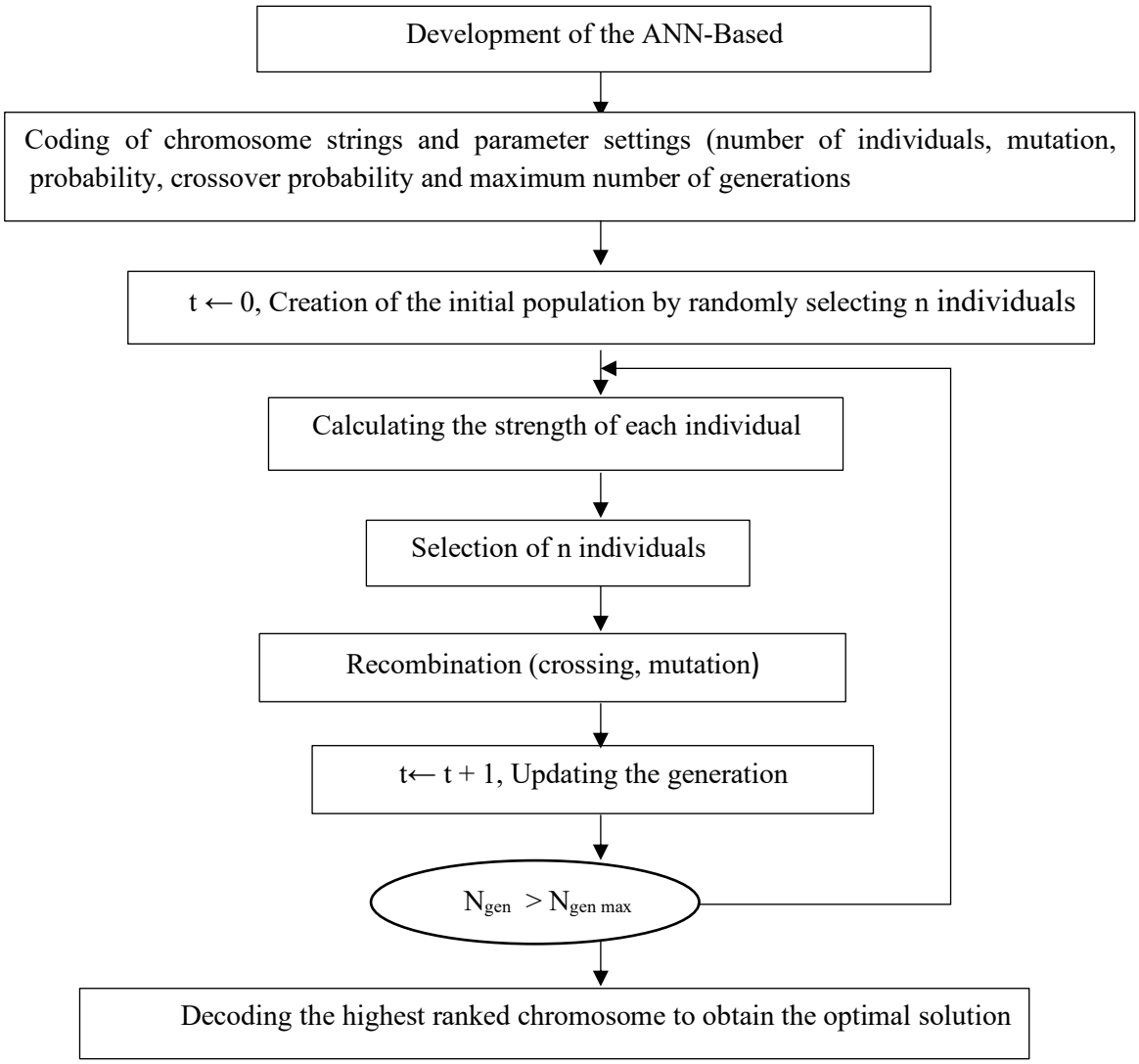

Figure 3: Block diagram of a genetic algorithm flow chart

2.3.4 Adsorption capacity of activated carbon

2.3.4.1 The iodine value

The iodine value is an important characteristic in the evaluation of activated carbon micropores and was determined using the method applied by Koné *et al* and Ahmed *et al* [13, 25]. Thus, a volume of 15 mL of a 0.2 N iodine solution is brought into contact with 0.05 g of activated carbon for 4 min. The treated solution was filtered and then 10 mL of filtrate was assayed with a 0.1 N sodium thiosulphate solution in the presence of a few drops of a 0.1 N starch solution. A blank test was carried out under the same conditions in the absence of activated carbon. Finally, the iodine value (I_d) expressed in mg/g was calculated by applying equation (1).

$$I_d = \frac{(Vb - Vs) \times N \times 126{,}9 \times \left(\frac{15}{10}\right)}{m} \qquad (7)$$

Where, V_b and V_s, the volumes (in mL) of sodium thiosulphate poured in during the blank test and the test with the adsorbent respectively; N, the normality of the sodium thiosulphate solution and m, the mass of the adsorbent (in g).

2.3.4.2 Methylene blue capacity

The adsorption capacity of methylene blue, which is an indicator of the mesoporosity of activated carbons, was determined by Konan *et al* and Bestani *et al* [12, 26]. The methylene blue adsorption tests were carried out by mixing 0.3 g of activated carbon with 100 mL of methylene blue solution at 1 $g.L^{-1}$. After stirring for 24 h, the mixture was filtered and the residual concentration of methylene blue was measured at 664 nm using a UV/VIS spectrophotometer. The adsorption capacity of Methylene Blue (I_{BM}) is given by the following formula:

$$I_{BM} = \frac{(C_i - C_r)}{m} \times V \quad (8)$$

C_i and C_r are the initial and residual concentrations of methylene blue (in $g.L^{-1}$); V, the volume (in L) of the methylene blue solution used for the adsorption tests and m, the mass (in g) of activated carbon.

2.3.5 Characterisation of activated carbons

Several methods were used to characterise the activated carbons obtained.

2.3.5.1 Zero charge point pH (pHpzc)

The nil charge point pH (pHpzc) which gives the net charge of the material surface was determined according to the method described by Konan *et al* [12]. A volume of 50 mL of NaCl solution (0.01 M) was introduced into the reactors containing 0.15 g of activated carbon to be analysed. The pH of each reactor is adjusted (variation of values between 2 and 12, in steps of 1) by adding 0.1 M NaOH or HCl solution. Stirring is maintained for 48 hours using a multi-stirring system, at a temperature of 25 °C. The contents of these reactors are then filtered through filter paper. The final pH of each mixture is then measured. The graph $\Delta pH = f(pH_i)$ is plotted, where $\Delta pH = (pH_f - pH_i)$. The pHpzc is defined as the point of intersection of the curve with the zero axis.

2.3.5.2 Spectroscopy IR-TF

The functions on the surface of activated carbons were determined by infrared spectroscopy.

2.3.5.3 Scanning Electron Microscopy (SEM) coupled with energy dispersive spectroscopy (EDS) of activated carbon

Scanning electron microscopy was used to study the surface morphology of activated carbon. A Hirox SH4000 M spectrophotometer was used for this purpose. This apparatus allows the evaluation of the morphology of the carbon. EDS analysis is an analytical method used to determine the chemical composition of the elements and to map the chemical elements present. The analysis was carried out at the laboratory of the University of Man/Cote d'Ivoire

2.3.5.4 Determination of pore texture, pore volume and pore diameter

The analysis of activated carbon pores was performed using Gold APP Instruments, V-Sorb 2800S. The nitrogen sorption method was applied. The specific surface area was evaluated by the Brunauer-Emmett-Teller (BET) multipoint. Pore volume and diameter were determined by the Barret, Joyner and Halenda (BJH) adsorption method. The analysis was done at the laboratory of the University of Man/Cote d'Ivoire.

2.3.5.5 Diffraction of activated carbon

The X-ray crystallographic analysis of the samples at room temperature was carried out using the EMPYREAN diffractometer type 11078671. The diffractometer is equipped with a goniometer with

Bragg Brentano geometry. In this type of diffractometer, a beam of X-rays is directed onto the sample being analysed and it is observed what is returned by diffraction, which is expressed through the equation :

$$\lambda = 2\ d\ \sin\theta \qquad (9)$$

Where,

λ : wavelength of the X-ray source ;
d : inter-reticular distance ;
θ: diffraction angle (Bragg angle).

3. Results and discussion

3.1 Screening of factors

The objective of this section is to identify the factors that can have an effect on the activated carbon preparation process. The iodine index was chosen as the answer. Table 6 gives the results obtained for each experiment carried out.

Table 6: Results obtained for the different experiments

Exp. N^0	Raw material	Chemical product	Concen-tration (mol.L^{-1})	Impregnation time (h)	Carbonization Temp. (°C)	Charring time (h)	**Iodine Index (mg.g^{-1})**
1	BHT	H_3PO_4	1	24	500	3	**513.945**
2	BMC	H_3PO_4	3	12	700	3	**723.330**
3	BMC	$ZnCl_2$	3	24	500	5	**513.945**
4	BHT	$ZnCl_2$	3	24	700	3	**856.575**
5	BMC	H_3PO_4	1	24	700	5	**818.505**
6	BHT	$ZnCl_2$	1	12	700	5	**875.610**
7	BHT	H_3PO_4	3	12	500	5	**647.190**
8	BMC	$ZnCl_2$	1	12	500	3	**380.700**

The coefficient of the polynomial model resulting from the Hadamar plan and their common standard deviation are presented in the Table 7.

Table 7: Different coefficients

	b_0	**b_1**	**b_2**	**b_3**	**b_4**	**b_5**	**b_6**	**Standard deviation**
Iodine Index	666.22	57.10	9.51	19.03	9.51	152.28	47.58	9.52

The different coefficients obtained range from 9.51 to 152.28 with a standard deviation of 9.52. By comparing the absolute value of the coefficients to their standard deviation, we find that *Hyphaene Thebaica* raw material, temperature and charring time (X_1, X_5 and X_6) influence the responses. The positive sign (+) of the coefficients b_2, b_3, and b_4 shows that the factors activating agent (X_2), activating agent concentration (X_3) and impregnation time (X_4) should be set at their high level (+1) to have a high iodine number corresponding to good microporosity. Thus, the rest of this work was carried out with the raw material based on *Hyphaene Thebaica* activated with 3 M H_3PO_4 for 24 h.

3.2 Full Factorial design results

The factors activation temperature and carbonisation duration were retained for the rest of our work. To improve the performance of the process on the quality of the activated carbons obtained, we chose as responses the iodine index (Y_1) to optimise the micropores and the methylene blue adsorption capacity (Y_2) to minimise the macropores. Table 8 shows the experimental matrix and the responses obtained.

Table 8: Matrix of experiments and responses

Exp. N°	X_1	X_2	Y_1 (mg.g^{-1})	Y_2 (mg.g^{-1})
1	-1	-1	532.980	114.744
2	1	-1	571.050	137.217
3	-1	1	723.330	193.627
4	1	1	799.470	287.343

The results of the 4 tests were modelled according to the first degree polynomial equation. This model is written in the following form:

$$Y = b_0 + b_1X_1 + b_2X_2 + b_{12}X_1X_2 \quad (10)$$

The processing of the above results has allowed us to obtain the different equations for each of the responses. The model equation for optimizing the micropores is written:

$$Y_{1\,(Iodine)} = 656.7075 + 28.5525\,X_1 + 104.6925\,X_2 + 9.5175\,X_1X_2 \quad (11)$$

The model equation for minimising the macropores is written:

$$Y_{2(MB)} = 183.2328 + 29.0473\,X_1 + 57.2523\,X_2 + 17.8107\,X_1X_2 \quad (12)$$

The quality of the developed model is evaluated on the basis of the determination coefficient (R^2), the adjusted determination coefficient (R^2_{adj}). **Table 9** ANOVA for full factorial design model.

Table 9: ANOVA for full factorial design model

Correlation coefficient	$Y_{1(Iodine)}$	$Y_{2(Methylene\ blue)}$
R^2	0.99 %	0.93 %
R^2_{adj}	0.97 %	0.79 %

The very good correlation between the experimental values and the predicted values is pointed out confirming that both models are valid [27].

3.3 Global optimisation of activated carbon preparation conditions using the genetic algorithm

This method was used to solve the complex equations (Eq 11 and 12) by maximising the formation of Y_1 micropores (iodine capacity) and minimising that of Y_2 macropores (methylene blue capacity). Figure 4 shows the optimisation curve. The optimal conditions for the preparation of activated carbons are: 500.850 °C carbonisation temperature; 4.99 hours for the carbonisation time; 723.649 mg.g^{-1} for the iodine index and 194.023 mg.g^{-1} for the adsorption capacity of methylene blue. These values were obtained by the coding calculation of the natural variables U and coded variables X by applying equations (3 and 4). Confirmatory tests were carried out on these optimum conditions to assess the performance of the activated carbons.

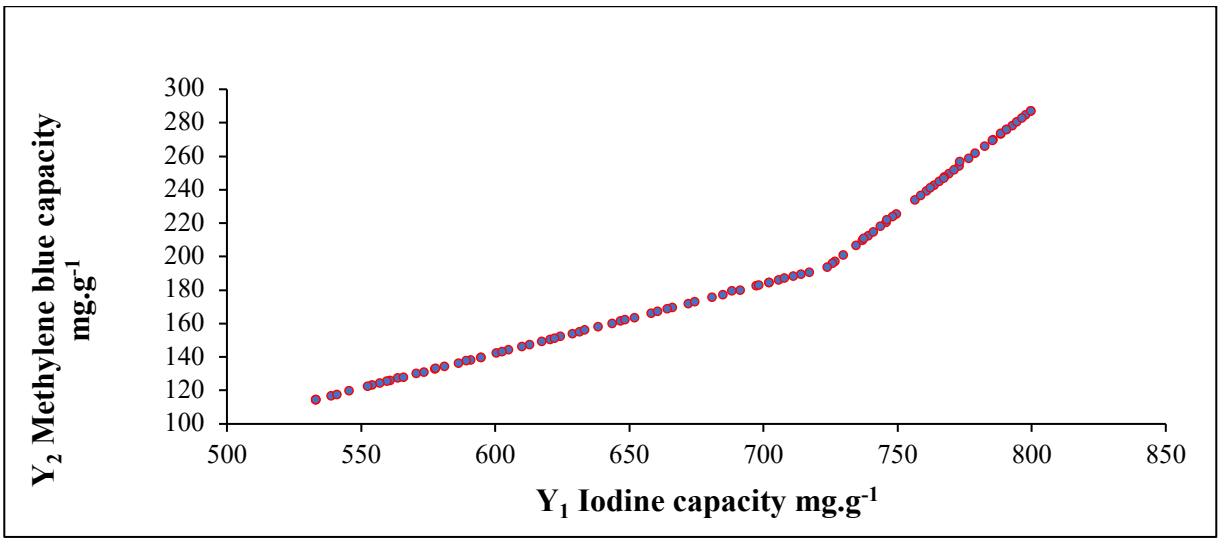

Figure 4: Optimization curve for micropores via genetic algorithm (Pareto front)

The activated carbon prepared from the optimal conditions has an iodine value of 710.640 $mg.g^{-1}$ and a methylene blue adsorption capacity of 188.009 $mg.g^{-1}$. The coefficients of variation (CV) between the experimental value and the calculated value are in the order of 1.830% and 3.198% for the iodine value and the methylene blue value respectively. These coefficients being lower than 5% [23], validate the linear model of the studied phenomenon.

4. Characteristics of activated carbon obtained under optimal conditions

4.1 Physical characteristics

Table 10 shows the physical characteristics of the activated carbon prepared after optimization

Table 10: Physical characteristics

Specific surface ($m^2.g^{-1}$)	Total pore volume ($cm^3.g^{-1}$)	Average pore diameter (nm)
705.615	0.906	1.66

The value of the specific surface obtained by the BET theory is 705.915 $m^2.g^{-1}$. This surface is characteristic of a good quality activated carbon. Indeed, the specific surface obtained belongs to the interval [500; 1500] $m^2.g^{-1}$. This surface is defined by the International Union of Pure and Applied Chemistry (IUPAC) to identify commercial activated carbons. Also, this surface is comparable to that found by Sanda [11] which is 722 $m^2.g^{-1}$ using the same precursor *Hyphaene Thebaica* and that found by Siragi *et al* [6] which is 727 $m^2.g^{-1}$ using activated carbon prepared with *Parinari Macrophylla*. In addition, the observation of the nitrogen adsorption/desorption isotherm curve at 77 K (Figure 5) indicates a type IV isotherm according to the classification of the International Union of Pure and Applied Chemistry (IUPAC). This type of isotherm characterises the simultaneous presence of micropores and mesopores suggesting that the activated carbon used would be both microporous and mesoporous. The *Hyphaene Thebaica* activated carbon has a pore volume of 0.906 $cm^3.g^{-1}$ and an average pore diameter of 1.66 nm.

4.2 Chemical characteristics

Table 11 shows the chemical characteristics of the activated carbon prepared after optimisation. The value of iodine value obtained in this study is in the same order of magnitude as that obtained in other studies [6,12]. The latter obtained values of 599 and 655.50 $mg.g^{-1}$ respectively.

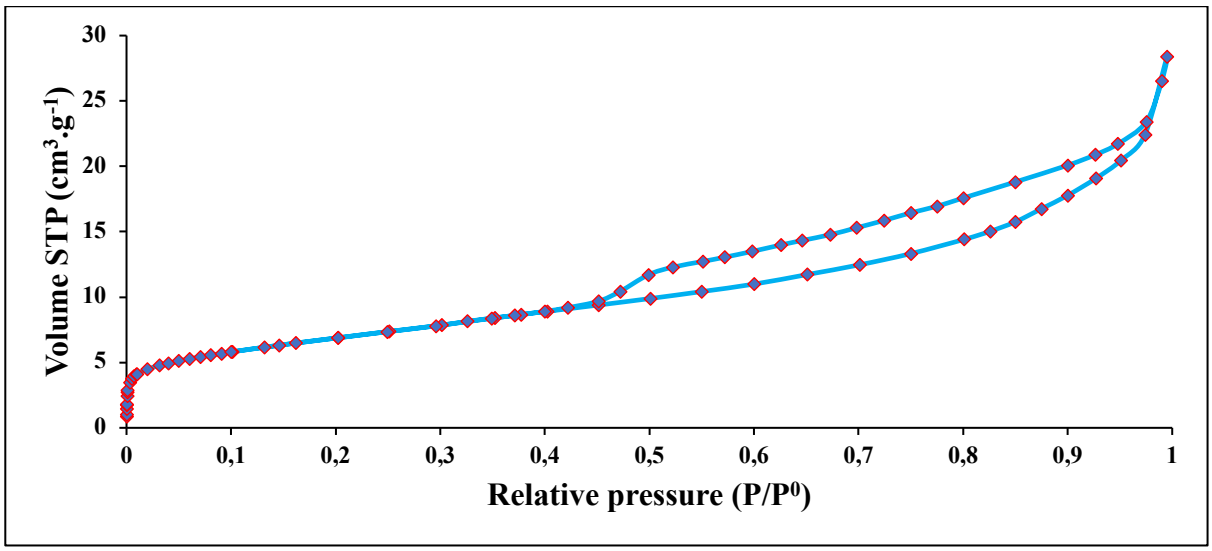

Figure 5: Isotherm of nitrogen adsorption/desorption at 77 K by activated carbon obtained under optimal conditions

Table 11: Chemical characteristics

Iodine index (mg.g^{-1})	Adsorption capacity of methylene blue (mg.g^{-1})	pHpzc
710.640	188.009	6

The methylene blue adsorption capacity value is comparable to that obtained by Briton *et al* [27] who obtained a value of 200 mg.g^{-1}. This value is higher than that obtained by other authors Koné *et al;* Bestani *et al* and Zakaria *et al* [13,26,28] As for the zero charge point pH (pHpzc) (Figure 6), the result shows that the prepared activated carbon is slightly acidic. Thus, the activated carbon will be anion attractive for a pH < 6 and cation attractive for a pH > 6.

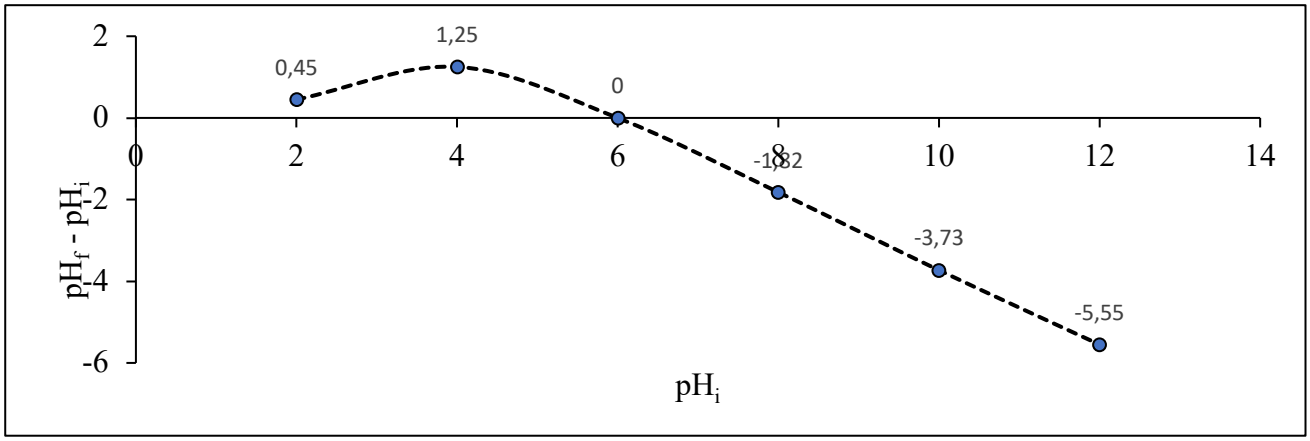

Figure 6: Determination curve of the zero charge point pH of activated carbon obtained under optimal conditions

4.3 Surface function

The infrared spectrum of the optimized activated carbon is shown in Figure 7. Analysis of the spectrum allowed the association of characteristic peaks with functional groups present on the surface of the activated carbon of *Hyphaene Thebaica* (AC-HT) obtained under the optimal conditions. Thus the peak observed at 745 cm^{-1} could be attributed to the O-H elongation vibration of aromatic compounds [13,29,30]. The peak at 868 cm^{-1} is due to out-of-plane strain mode of C-H for different substituted

benzene rings. Another C-H elongation vibration, was observed at wavelengths 2653-3587 cm^{-1}. Possible chemical compounds would be quinones [13]. As for the carbonyl function was identified by the peak at 1700 cm^{-1} corresponding to a C=O stretching vibration.

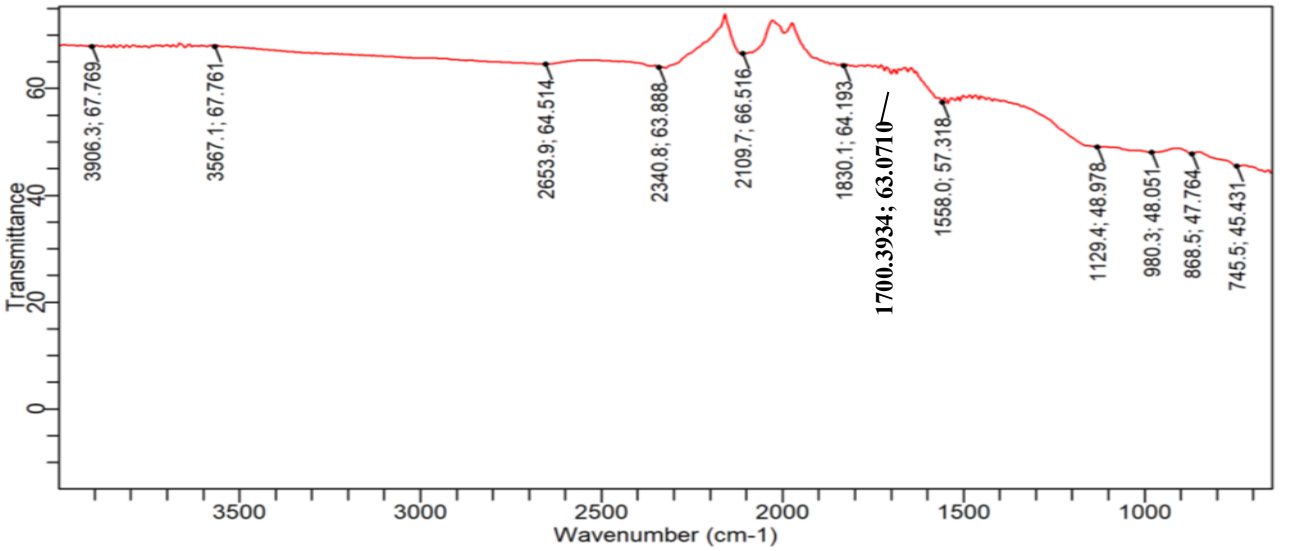

Figure 7: Infrared spectrum of activated carbon obtained under optimal conditions

4.4 Scanning electron microscopy (SEM) coupled with energy dispersive spectroscopy (SEM/EDS) of activated carbon

The photograph shows that the activated carbon *Hyphaene Thebaica* (AC-HT) is porous. This porosity consists of pores of different sizes. On the one hand, one can observe smaller pores that could be micropores (figure 8a) and on the other hand larger pores that could be mesopores or even macrospores (figure 8b).

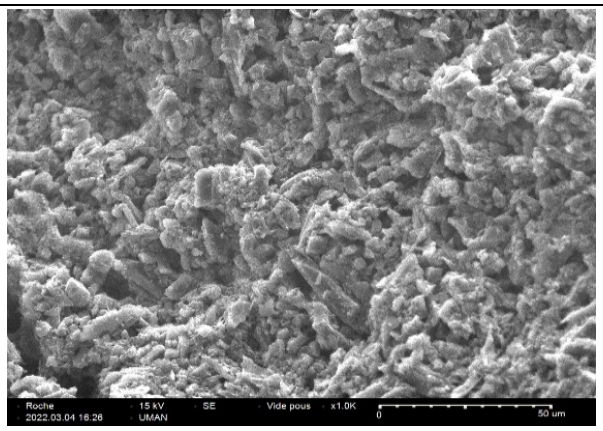

(8a)

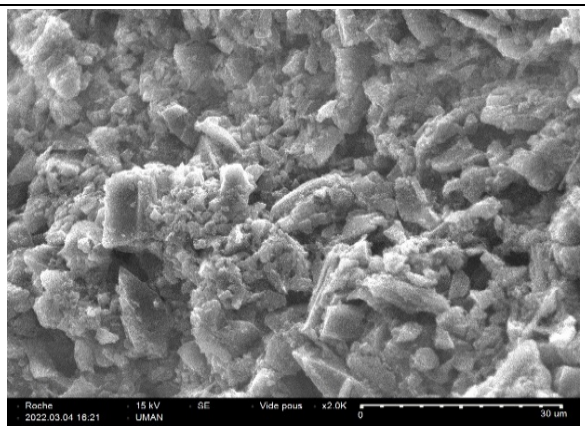

(8b)

Figure 8: Scanning electron microscopy (SEM) of activated carbon obtained under optimal conditions

This morphology composed of several pores was observed by [13] who used branches of Borassus Aethiopum. In addition, the charcoal contains functional groups (O-H, C=O, C-H) on the IR spectrum at specific wavelengths. These results are in agreement with the EDS chemical mapping, which reveals the presence of the element oxygen. The high carbon content of 71.79% shows that Hyphaene Thebaica shells are rich in lignite and suitable for the production of quality activated carbon. The presence of the chemical element P, detected in EDS, would come from H_3PO_4 used for the activation of the residual

quantities of this chemical agent that remained in the activated carbon after the washing stage. The presence of the chemical element P, detected in EDS, would come from H_3PO_4 used for the activation of the residual quantities of this chemical agent having remained in the activated carbon after the washing stage. As regards the elements Fe and Al, their presence probably comes from the biomass because they are inorganic elements that are very common in the chemical composition of lignocellulosic biomass (figure 9).

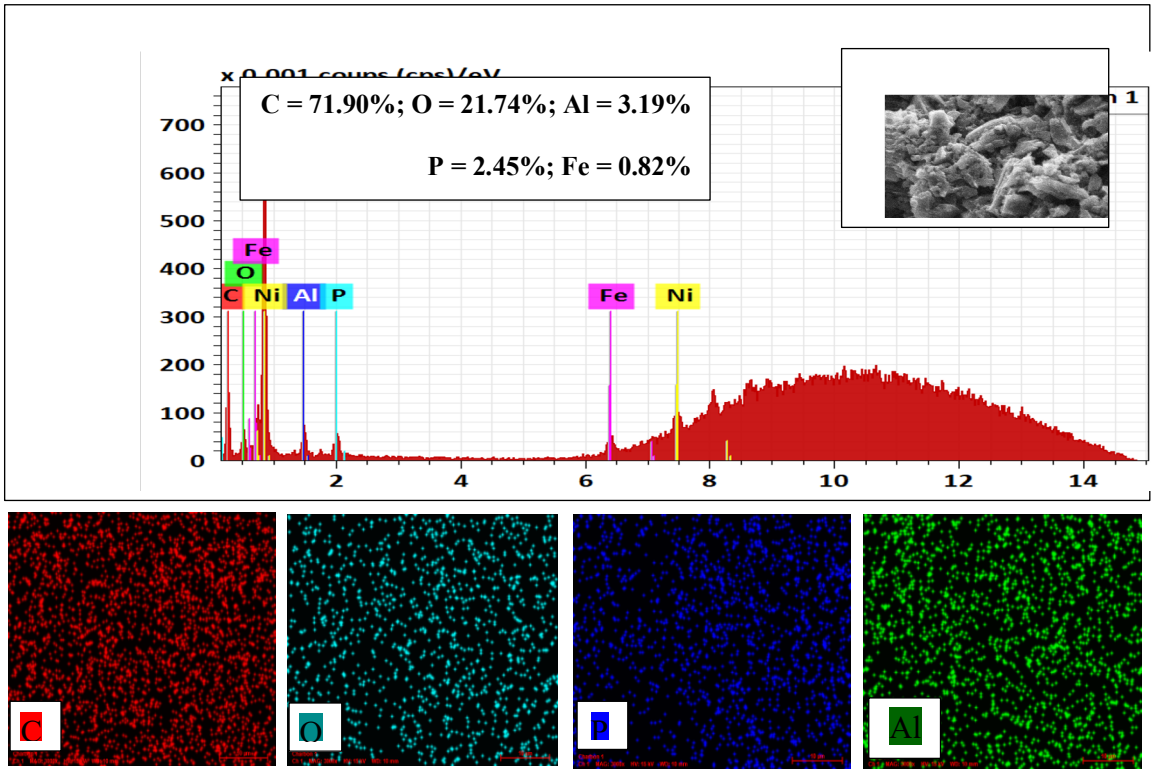

Figure 9: Energy dispersive X-ray spectrum (EDS) and chemical element mapping of activated carbon obtained under optimal conditions

4.5 X-ray diffraction

The diffractogram of the optimised activated carbon is shown in Figure 10. The X-ray diffraction pattern of the activated carbon *Hyphaene Thebaica* (AC-HT) (Figure 10) shows two peaks around 24.12 and 43.26 degrees corresponding to a reflection of a disordered stacking of micro graphites [31].

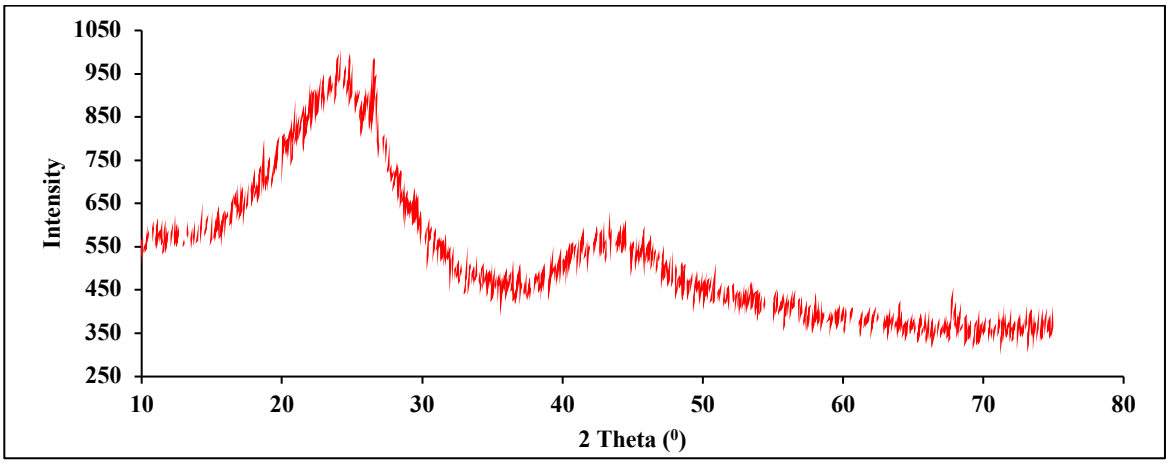

Figure 10: Diffractogram of activated carbon obtained under optimal condition

The width of the peaks indicates the amorphous nature of the carbon. This would be characteristic of an amorphous activated carbon.

Conclusion

This study has shown that *Hyphaene Thebaica* shells are interesting precursors for the preparation of microporous activated carbon by the two-step chemical method of orthophosphoric acid (H_3PO_4) activations. The full factorial design via the genetic algorithm was used to determine the optimal preparation conditions: 500.850°C carbonization temperature; 4.99 hours carbonization time; 723.649 mg/g iodine value; 194.023 mg/g methylene blue adsorption capacity and the raw material based on *Hyphaene Thebaica* activated with 3 M H_3PO_4 for 24 h. The values of diode number 710.640 $mg.g^{-1}$ and methylene blue adsorption capacity 188.009 $mg.g^{-1}$ obtained show that the activated carbon prepared under optimal conditions is very efficient to adsorb these two molecules in aqueous solution. Thus, this activated carbon could be produced on a large scale and used to remove organic or inorganic pollutants from wastewater by adsorption.

Acknowledgements: The authors would like to thank the World Bank, French Agency for Development and the African Centre of Excellence for Waste to Value (CEA-VALOPRO) for their invaluable financial support for this research. In accordance with ethical standards.

Disclosure statement: *Conflict of Interest:* The authors declare that there are no conflicts of interest. *Compliance with Ethical Standards:* This article does not contain any studies involving human or animal subjects.

References

[1] C. Balogoun, M. Bawa, S. Osseni, M. Aina, « Préparation des charbons actifs par voie chimique à l'acide phosphorique à base de coque de noix de coco », *Int. J. Bio. Chem. Sci*, 9 (2015) 563, doi: 10.4314/ijbcs.v9i1.48.

[2] S. D. B. Maazou, H. I. Hima, M. M. Malam Alma, Z. Adamou, I. Natatou, « Elimination du chrome par du charbon actif élaboré et caractérisé à partir de la coque du noyau de *Balanites aegyptiaca* », *Int. J. Bio. Chem. Sci*, 11 (2018) 3050, doi: 10.4314/ijbcs.v11i6.39.

[3] M. baye Gueye, « Développement de charbon actif à partir de biomasses lignocellulosiques pour des applications dans le traitement de l'eau », These de Doctorat en Energie, Institut International de l'Ingenierie de l'Eau et de l'Environnement, (2015) 232.

[4] J. Jagiello, J. Kenvin, A. Celzard, V. Fierro, « Enhanced resolution of ultra micropore size determination of biochars and activated carbons by dual gas analysis using N_2 and CO_2 with 2D-NLDFT adsorption models », *Carbon*, 144 (2019) 206-215, doi: 10.1016/j.carbon.2018.12.028.

[5] M. L. Sekirifa, M. Hadj-Mahammed, S. Pallier, L. Baameur, D. Richard, A. H. Al-Dujaili, « Preparation and characterization of an activated carbon from a date stones variety by physical activation with carbon dioxide », *Journal of Analytical and Applied Pyrolysis*, 99 (2013) 155‑160, doi: 10.1016/j.jaap.2012.10.007.

[6] M. Siragi D. B., D. Desmecht, H. I. Hima, O. S. Mamane, I. Natatou, « Optimization of Activated Carbons Prepared from <i>Parinari macrophylla</i> Shells », *MSA*, 12 (2021) 207-222, doi: 10.4236/msa.2021.125014.

[7] M. A. A. Zaini, L. L. Zhi, T. S. Hui, Y. Amano, M. Machida, « Effects of physical activation on pore textures and heavy metals removal of fiber-based activated carbons », *Materials Today: Proceedings*, 39 (2021) 917‑921, doi: 10.1016/j.matpr.2020.03.815.

[8] O. Oginni, K. Singh, G. Oporto, B. Dawson-Andoh, L. McDonald, E. Sabolsky, « Effect of one-step and two-step H_3PO_4 activation on activated carbon characteristics », *Bioresource Technology Reports*, 8 (2019) 100307, doi: 10.1016/j.biteb.2019.100307.

[9] O. Oginni, K. Singh, G. Oporto, B. Dawson-Andoh, L. McDonald, E. Sabolsky, « Influence of one-step and two-step KOH activation on activated carbon characteristics », *Bioresource Technology Reports*, 7 (2019) 100266, doi: 10.1016/j.biteb.2019.100266.

[10] S. Das et S. Mishra, « Box-Behnken statistical design to optimize preparation of activated carbon from Limonia acidissima shell with desirability approach », *Journal of Environmental Chemical Engineering*, 5 (2017) 588‑600, doi: 10.1016/j.jece.2016.12.034.

[11] O. Sanda Mamane, « Valorisation de déchets agro-alimentaires pour l'élaboration de charbons actifs ; caractérisation et application dans la dépollution des eaux usées chargées en chrome issues de la Tannerie Malam Yaro de Zinder-Niger », These de Doctorat Chimie Minerale de Metaux, Université Abdou Moumouni de Niamey, (2019) 176.

[12] A. T. S. Konan, R. Richard, C. Andriantsiferana, K. B. Yao, « Recovery of borassus palm tree and bamboo waste into activated carbon: application to the phenolic compound removal », *Journal of Materials and Environmental Science,* 11 (2020) 1584-1598.

[13] H. Koné, K. E. Kouassi, A. S. Assémian, K. B. Yao, P. Drogui, « Investigation of breakthrough point variation using a semi-industrial prototype packed with low-cost activated carbon for water purification », *Journal of Materials and Environmental Science,*12 (2021) 224-243.

[14] A. T. S. Konan, « Couplage adsorption/procédé d'oxydation avancée pour l'élimination du 2,4-diméthylphénol en milieu aqueux », These en Genie des Procedés, Institut National Felix HOUPHOUET BOIGNY et Université de Toulouse, (2019) 209.

[15] D. Bamba, « Elimination du diuron des eaux par des techniques utilisant les ressources naturelles de la cote d'Ivoire : photocatalyse solaire et charbon actif de coques de noix de coco », These de Doctorat Chimie-Physique, Université de Cocody Abijan, (2009) 194.

[16] N. Aboua Kouassi, « Optimisation par le plan Factoriel complet des conditions de production de charbon actif et utilisation pour l'élimination de colorant et métaux lourds en solutions aqueuses », These de Doctorat Chimie-Physique, Université F. Houphouet Boigny, (2013) 194.

[17] K. K. Naganathan, A. N. M. Faizal, M. A. A. Zaini, A. Ali, « Adsorptive removal of Bisphenol a from aqueous solution using activated carbon from coffee residue », *Materials Today: Proceedings*, 47 (2021) 1307-1312, doi: 10.1016/j.matpr.2021.02.802.

[18] H. N. Tran, S.-J. You, H.-P. Chao, « Fast and efficient adsorption of methylene green 5 on activated carbon prepared from new chemical activation method », *Journal of Environmental Management*, 188 (2017) 322-336, doi: 10.1016/j.jenvman.2016.12.003.

[19] A. Supong, P. C. Bhomick, M. Baruah, C. Pongener, U. B. Sinha, D. Sinha, « Adsorptive removal of Bisphenol A by biomass activated carbon and insights into the adsorption mechanism through density functional theory calculations », *Sustainable Chemistry and Pharmacy*, 13 (2019) 100159, doi: 10.1016/j.scp.2019.100159.

[20] J. Ano, A. S. Assémian, Y. A. Yobouet, K. Adouby, P. Drogui, « Electrochemical removal of phosphate from synthetic effluent: A comparative study between iron and aluminum by using experimental design methodology », *Process Safety and Environmental Protection*, 129 (2019) 184‑195, doi: 10.1016/j.psep.2019.07.003.

[21] A. E. Armand, Y. Y. Augustin, K. Y. Urbain, T. Albert, « et caractérisation physico-chimique », *International Journal of innovation and Applied Studies*, 29 (2020) 1161-1171.

[22] J. Ano, B. G. Henri Briton, K. E. Kouassi, K. Adouby, « Nitrate removal by electrocoagulation process using experimental design methodology: A techno-economic optimization », *Journal of Environmental Chemical Engineering*, 8 (2020) 104292, doi: 10.1016/j.jece.2020.104292.
[23] L. Y. Ouattara *et al.*, « Optimization of the autoclave-assisted alkaline delignification of cocoa (Theobroma cacao) pod husks using KOH to maximize reducing sugars », *BioRes*, 17 (2021) 826‑848, doi: 10.15376/biores.17.1.826-848.
[24] Y. K. Benjamin, E. A. Nogbou, G. Ado, C. Azzaro-Pantel, A. Davin, « Modeling and Optimization of M-cresol Isopropylation for Obtaining N-thymol: Combining a Hybrid Artificial Neural Network with a Genetic Algorithm », *International Journal of Chemical Reactor Engineering*, 5 (2007) 14, doi: 10.2202/1542-6580.1605.
[25] M. J. Ahmed & S. K. Dhedan, « Equilibrium isotherms and kinetics modeling of methylene blue adsorption on agricultural wastes-based activated carbons », *Fluid Phase Equilibria*, 317 (2012) 9‑14, doi: 10.1016/j.fluid.2011.12.026.
[26] B. Bestani, N. Benderdouche, B. Benstaali, M. Belhakem, et A. Addou, « Methylene blue and iodine adsorption onto an activated desert plant », *Bioresource Technology*, 99 (2008) 8441‑8444 doi: 10.1016/j.biortech.2008.02.053.
[27] B. G. H. Briton, B. K. Yao, Y. Richardson, L. Duclaux, L. Reinert, Y. Soneda, « Optimization by Using Response Surface Methodology of the Preparation from Plantain Spike of a Micro-/Mesoporous Activated Carbon Designed for Removal of Dyes in Aqueous Solution », *Arab J Sci Eng*, 45 (2020) 7231‑7245, doi: 10.1007/s13369-020-04390-0.
[28] R. Zakaria, N. A. Jamalluddin, M. Z. Abu Bakar, « Effect of impregnation ratio and activation temperature on the yield and adsorption performance of mangrove based activated carbon for methylene blue removal », *Results in Materials*, 10 (2021) 100183, doi: 10.1016/j.rinma.2021.100183.
[29] A. Mamaní, M. F. Sardella, M. Giménez, C. Deiana, « Highly microporous carbons from olive tree pruning: Optimization of chemical activation conditions », *Journal of Environmental Chemical Engineering*, 7 (2019) 102830, doi: 10.1016/j.jece.2018.102830.
[30] S. Yorgun & D. Yıldız, « Slow pyrolysis of paulownia wood: Effects of pyrolysis parameters on product yields and bio-oil characterization », *Journal of Analytical and Applied Pyrolysis*, 114 (2015) 68‑78, doi: 10.1016/j.jaap.2015.05.003.
[31] H. Soni & P. Padmaja, « Palm shell based activated carbon for removal of bisphenol A: an equilibrium, kinetic and thermodynamic study », *J Porous Mater*, 21 (2014) 275‑284, doi: 10.1007/s10934-013-9772-5.